Eng Int Syst (2023) 1: 43–52

Engineering
Intelligent Systems

Regional Surface Deformation Monitoring Method Based on GNSS and Satellite Signal Processing

Liang Wang*

College of Urban and Rural Construction, Shaoyang University, Shaoyang 422000, China

In order to reduce the monitoring error of vertical displacement and horizontal displacement in surface deformation, a regional surface deformation monitoring method based on GNSS and satellite signal processing is proposed. According to the basic principle of coordinate rotation transformation, the off set problem existing in the inflection point is adjusted at the same time to make the theoretical coordinate system rotate into the coordinate system in real mining. According to the GNSS and satellite signal processing results, the original working surface is adjusted to the calculated working surface to achieve the segmentation and prediction of the working surface and the monitoring of the regional surface deformation.According to the engineering geological and hydrogeological conditions, NNBR model is introduced to measure and calculate the surface settlement due to the construction of tunnelling shield, and the design of regional surface deformation monitoring program is completed. The experimental results show that the monitoring value of the designed method is very close to the measured value of the vertical displacement, the monitoring error for surface horizontal displacement is low, and the monitoring value of regional surface settlement is basically consistent with the real value.

Keywords: GNSS; Satellite signal processing; Regional surface deformation; Deformation monitoring method

1. INTRODUCTION

Deformation refers to the change of the shape, size and position of an entity in time and space. This change is acceptable within a certain range. Once it exceeds a certain value, it may cause disasters [1]. For example, for cities built in the lower reaches of rivers, because industries consume massive amounts of groundwater, this will affect the structure of underground soil layer and cause land subsidence. Also, underground mining will cause land subsidence [2,3]. Therefore, in order to ensure the sustainable development of a mining area [4], advanced technology must be used to timely monitor and control the damage caused by land subsidence. Effective, real-time monitoring of a mining area can timely find the subsidence law and change trend of the surface, provide very effective early warning for the safe operation and environmental damage of the mining area, and strengthen the comprehensive treatment of the subsiding area [5]. Therefore, the real-time monitoring of regional surface deformation is of great significance to the development of society and the national economy.

Now MEMS (micro electro mechanical system) has the advantages of low cost, small volume, low power consumption, high integration and impact resistance. It has broad application prospects in military, industrial equipment, electronic products and other fields. The inertial measurement system is used to monitor the surface subsidence and deformation caused by mining, as it can quickly obtain the change in spatial position and the degree of change within the entire deformation area, so as to control the surface subsidence in the monitored area. Multiple Mimus (micro inertial

*Email of corresponding author: 3508@hnsyu.edu.cn

measurement units) are selected to design the distribution network and construct the monitoring system, so as to provide a large amount of monitoring data for the analysis of surface deformation and obtain comprehensive and intuitive results. Several researchers have conducted in-depth studies on this. A new surface deformation monitoring algorithm based on small baseline differential SAR inter ferogram was applied to monitor the time evolution of surface deformation [6]. The proposed technique combines the differential interferograms generated by data pairs with small orbital spacing to limit the phenomenon of spatial correlation. The application of the singular value decomposition method can easily "link" independent SAR-acquireddata sets separated by large baselines, so as to improve the sampling rate of observation time. The availability of spatial and temporal data in the processed data is used to identify and filter atmospheric phase artifacts. Aldao et al. [7] asserted that in aviation maintenance tasks, it is very important to compare the measurements of aerospace deformation obtained by the monitoring lidar and by the photogrammetry system, and to inspect the fuselage and aerodynamic surface.Traditionally, this work has been carried out by maintenance personnel who manually inspect all parts of the fuselage, which is a huge cost for airlines. This paper evaluates the feasibility of implementing a low-cost portable 3D scanning system that can easily and accurately perform these inspection tasks. In this paper, systems are compared: alidar Kinect one sensor and a Sony Alpha 6000 digital camera using photogrammetry software and a stereo camera.Their functions and their main shortcomings are examined to determine which technology is suitable for the inspection of aviation craft surfaces. The Kinect lidar sensor shows the more promising results and offers the possibility of applying this technology to aircraft maintenance tasks in the future. Based on the above research, a regional surface deformation monitoring method based on GNSS and satellite signal processing is proposed. GNSS, the global satellite navigation system, is one of the important standards used to measure the level of national scientific and technological development and national defense strength. With the gradual improvement of the Beidou satellite navigation system, appropriate Beidou navigation technologies, services and products are more and more widely being used in various fields of daily life. The design and implementation of a multi-functional GNSS signal for the monitoring of regional surface deformation, provides a simulation signal and test environment for Beidou receiver for function verification and performance testing, and realizes the closed-loop testing and verification between receiver and simulator. It has great reference value for research engineering,and improves the performance of regional surface deformation monitoring methods.

2. REGIONAL SURFACE DEFORMATION MONITORING BASED ON GNSS AND SATELLITE SIGNAL PROCESSING

2.1 Coordinate Rotation Transformation

Through GNSS and satellite signal processing, when calculating the surface deformation parameters [8,9], the (x, y) coordinate system with x axis parallel to the strike main section and y axis parallel to the inclined main section is usually adopted, but in reality, the coordinate data will have different coordinate forms. Therefore, it is necessary to convert the coordinate position before monitoring the surface deformation to adjust the corner coordinates of the working surface to relative coordinates [10] prior to monitoring the regional surface deformation. The coordinate rotation transformation is represented by Formula (1):

$$\begin{aligned} x &= x^{'} \cos\theta + y^{'} \sin\theta \\ y &= x^{'} \sin\theta - y^{'} \cos\theta \end{aligned} \tag{1}$$

In Formula (1), the new coordinate points are represented by x and y, while the original coordinate points are represented by $x^{'}$ and $y^{'}$; When the $x^{'}$ axis of the original coordinate system rotates counterclockwise to the x axis of the new coordinate system, the angle value is represented by θ, and θ also represents the azimuth of the strike direction. Due to the technical limitations of satellite remote-sensing sensors, the visible light and near-infrared bands on the sensor have high resolution. However, this presents a problem: the surface temperature data obtained by using the thermal infrared band data with low spatial resolution on the same load is lacking in details. For example, the retrieved visible light and infrared data are not equal, so it is necessary to convert the spatial scale of surface temperature measurement to eliminate this issue. The coordinate rotation transformation of regional surface means that the identification, inference and prediction of surface temperature can span the geographical range and spatial resolution. The coordinate rotation transformation can be upscale and downscale. The scale can be arranged from point scale to global scale, consisting of several levels of observed data. The downscaling process involves actually refining the spatial resolution [11]. Within a certain spatial range, the data in the geographical range of low spatial resolution and large scale is deduced and displayed in the form of high spatial resolution and a small-scale geographical range. After this conversion, the data obtained via remote sensing can be richer. In this paper,the main purpose of coordinate rotation transformation is to refine the spatial resolution affected by surface temperature; that is, by downscaling the surface temperature.Downscaling is actually aggregating the trend surface factor of remote sensing spectral data from the high-scale S_H where the spatial resolution is located to the low-scale S_L. The relationship between the trend surface factor of low-scale S_L remote sensing spectral data and remote sensing L_{ST} products is as follows:

$$L_{ST_L} = f_L(S_{I_{L1}}, S_{I_{L2},\ldots}) \tag{2}$$

In Formula (2), L_{ST_L} represents the L_{ST} value estimated on the low-scale S_L, f_L represents the coordinate rotation transformation function, S_{l_L} represents the remote-sensing spectral data on the low-scale S_L, and the coordinate rotation transformation function can convert the remote sensing spectral data into L_{ST} function.In Formula (2), it is mainly due to the scale invariance between trend surface factor and L_{ST}, that is, the conversion function applicable to high-scale S_H can also be applied to low-scale S_L. As long as the remote sensing spectral indexes on the two scales are connected,

the conversion from trend surface factor to L_{ST} can also be completed.The direction of the off set of the coordinate system is adjusted to provide the direction of the offset of the subsequent operation.

2.2 Inflection Point Offset Processing

When the inflection point caused by cantilever force is off set, the off set length is the inflection point off set. However, in the case of surface deformation in an underground mining area, there are usually arbitrary polygon changes, so the inflection point off set will be greatly affected. Therefore, according to GNSS and satellite signal processing calculation, the inflection point off set s_x and s_y along the strike and dip direction of the working surface can be obtained [12].

By means of addition and subtraction, the offset distance of the inflection point in the strike direction can be calculated, although the inclination direction is influenced by the inclination of the resource layer.Therefore, the y coordinate of the corner point needs to be adjusted according to Formula (3):

$$y_m = y - s_x \cos\lambda - (h + s_y \sin\alpha) \times \cot\lambda \qquad (3)$$

In Formula (3), y_m represents the coordinates after adjustment, y represents the coordinates before adjustment, h represents the mining depth of the corner area, and λ represents the dip angle of the coal seam.

2.3 GNSS and Satellite Signal Processing

According to the results obtained by the inflection point offset process described above, GNSS and satellite signal processing are proposed, which is a wireless packet data exchange and data transmission technology [13]. This technology uses the time slot of GSM, and the normal data transmission rate is 61.7Kb/s, up to 178.4Kb/s. At the same time, GNSS has fast access speed. When users need a clear address channel, GNSS can provide services to users at any time. After mobile users complete the login operation, GNSS will always be online or in the process of connecting with users, and can be online in real time. The regional surface deformation monitoring method designed in this paper adopts GNSS communication technology, and the monitoring system will always incorporate a GNSS network. After logging in to the monitoring system, the staff can send and receive all the data about the regional surface in real time, and timely determine the local surface water and soil loss according to the data indicators of regional surface deformation. The flow of GNSS and satellite signal processing designed in this paper is shown in Figure 1.

As shown in Figure 1, firstly, the sediment content of surface runoff is collected. The collection module of the monitoring method is used to collect three kinds of data: sediment volume of surface runoff and sediment, rainfall and total runoff in the first two days, and in the last two days. During the collection process, it is necessary to ensure that there is no interference from other factors, so as to ensure the integrity and authenticity of the collected data.

Then, after the data acquisition process is completed, the remote real-time transmission is carried out through GNSS communication technology, and the obtained data is stored in the database of the monitoring system. The communication module of the monitoring system belongs to the access terminal equipment and supports the wireless packet transfer mode and GNSS communication network. The staff can directly connect with GNSS by means of mobile devices. The network TCP/IP protocol is embedded in the GNSS communication network. The data can be transmitted by establishing a connection between GNSS and the monitoring system. During transmission, the terminal equipment and the network server specify a transmission IP address and connect with the terminal equipment through the transmission channel. After receiving the request for data transmission, connection is made with the server according to the blocking receiving method. At this time, the data packet can be sent and received online in real time. After the uploaded data packet has been received, it can be parsed according to the TCP/IP protocol format, Finally, the parsed data is stored in the database of the monitoring system.

Finally, the runoff and sediment data is displayed and analyzed. The runoff and sediment data stored in the database is extracted and displayed in a list, or the runoff and sediment data and other data can be displayed in Excel format using the export key on the computer screen. The data in the table is screened according to relevant conditions, and the screening results are represented by an enlarged curve. Then, the staff analyze the original runoff and sediment data in the table and the change law reflected in the curve to enable them to observe and understand the connection state and working state of the monitoring equipment, in order to conduct timely maintenance. By analyzing the runoff and sediment data, staff can understand the state of surface runoff and sediment, determine the water situation and the soil loss, and take preventive measures in time.

2.4 Regional Surface Deformation Monitoring Process

By adjusting the original working surface to the calculated working surface, the segmentation prediction of the working surface is realized. The section line-filling algorithm is selected to segment the working surface [14], which the algorithm can do quickly and effectively,converting the working surface into a series of small rectangles (segments) for subsequent calculation. Then, these rectangles re super imposed to form the predicted value of surface deformation. The monitoring steps are shown in Figure 2.

3. REGIONAL SURFACE DEFORMATION MONITORING METHOD

(1) Engineering geological conditions

The soil of the stratum where the tunnel body is located is comprised mainly of a clay layer, silty clay layer, silt and sandy soil.

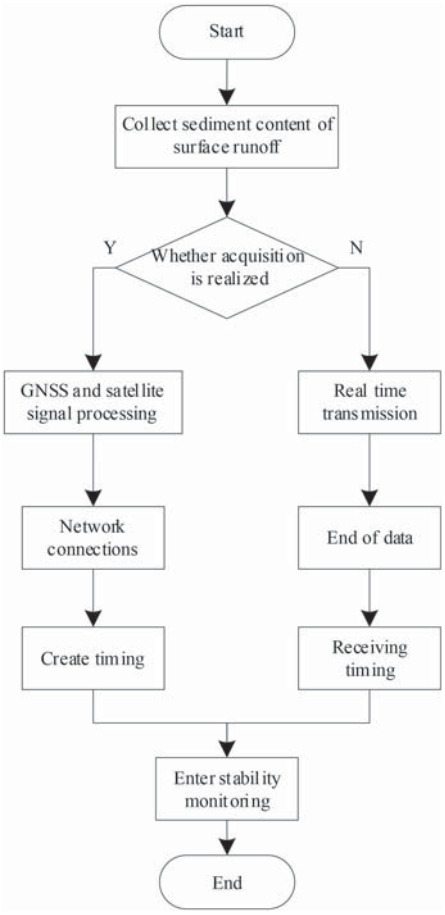

Figure 1 GNSS and satellite signal processing flow.

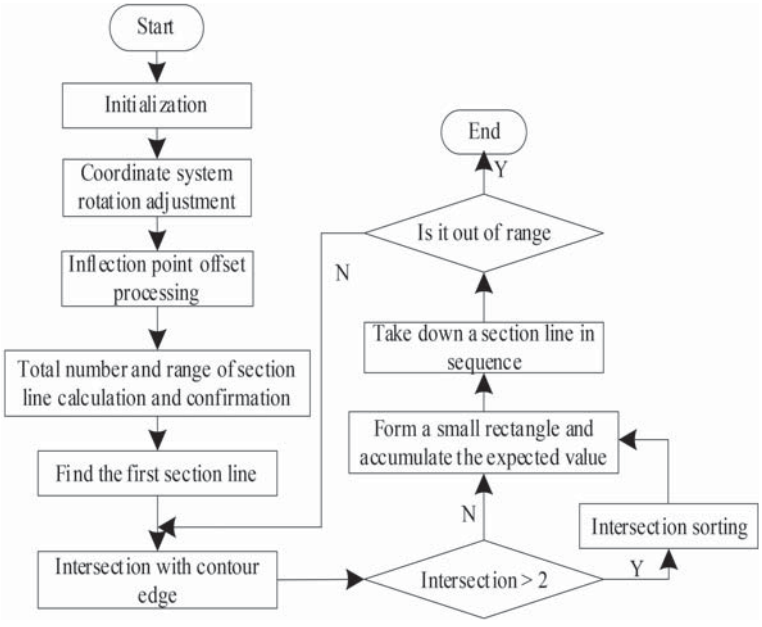

Figure 2 Monitoring of regional surface deformation.

(2) Hydrogeological conditions

Based on the relevant data obtained by geological exploration, there are five layers of groundwater within the scope of the project: one layer of stagnant water, two layers of phreatic water, and two layers of interlayer water. They are all distributed in the tunnel body area, and the interlayer water has micro pressure bearing characteristics. The geology of the water-resisting layer between the upper stagnant water and the first layer of phreatic water are mainly clay and silty clay, and the stratum presents an intermittent distribution state, with

Table 1 Groundwater level.

Type	Stable groundwater level		Aquifer
	Buried depth of water level/m	Water level elevatlon/m	
Upper stagnant water	1.10–3.80	31.31–33.54	Silt
	6.10–7.90	26.75–28.55	Silt and sand
Diving	10.50–15.00	19.54–22.24	Sand
	20.30–25.50	9.14–13.71	Sand
Interlayer water	29.20–31.90	2.75–6.23	Sand

poor overall continuity. The geology of phreatic water layer and interlayer water interval layer are mainly silty clay and a little clay. At the same time, the stratum is widely distributed and has good continuity. In addition, the buried depth of the perched water level in the upper layer is 1.10 to 3.80M, the buried depth of phreatic water level in the first layer is 6.1 to 7.9m, the buried depth of phreatic water level in the second layer is 10.5 to 15.0m, the buried depth of water level between the first layer is 20.3m to 25.5m, and the buried depth of water level between the second layer is 29.2 to 31.9m. The details of the groundwater level are shown in Table 1.

Based on the survey data and the collected hydrogeological data, the highest water level of the site over the years is close to the natural ground. The basic conditions for groundwater recharge, runoff and discharge are as follows: the main sources of the perched water in the upper layer are atmospheric precipitation, irrigation and lateral runoff, and the perched water in the upper layer discharges by means of evaporation and downward overflow. The interlayer water is mainly supplied by lateral runoff and overflow, and discharged by downward overflow.

3.1 Measurement and Calculation of Ground Settlement During Tunnelling Shield Construction

Based on the analysis of actual data above, the NNBR model is proposed to measure and determine surface settlement during tunnelling shield construction. The NNBR model is a similarity prediction method. It operates according to the basic principle of generating similar results by means of similar factors, detecting the most similar ones in the historical sample set, or taking several samples as the calculation results. This is a nonlinear calculation method.

The calculation factor set $x = (x_1, \cdots, x_m)$ consists of several main factors, and the corresponding results are taken as the calculation object sample y. A total of n samples are selected. The constructed matrix is as follows:

$$X_{n\times m} = \begin{Bmatrix} x_1 \\ x_2 \\ \vdots \\ x_n \end{Bmatrix} = \begin{Bmatrix} x_{11} & x_{12} & \cdots & x_{1m} \\ x_{21} & x_{22} & \cdots & x_{2m} \\ \vdots & \vdots & \ddots & \vdots \\ x_{n1} & x_{n2} & \cdots & x_{nm} \end{Bmatrix} \quad (4)$$

$$y = \begin{Bmatrix} y_1 \\ y_2 \\ \vdots \\ y_n \end{Bmatrix} \quad (5)$$

The real-time data x_{n+1} with a known factor can calculate the similarity between the calculation result and the y_i of y_{n+1} historical calculation object according to the distance between the historical sample $x_i (i = 1, \cdots, n)$ and x_{n+1}. The typical distance D_r expression is:

$$D_r = \left[\sum_{k=1}^{m} (x_{ik} - x_{(n+1)k})^2\right]^{1/2} \quad (i = 1, \cdots, n) \quad (6)$$

In Formula (6), n represents the number of historical samples, m represents the number of calculation factors, x_{ik} represents the k calculation factor in the i historical sample, and $x_{(n+1)k}$ represents the k calculation factor of the real-time calculation sample.

Arrange $r_{i,n+1}$ from small to large, find the historical sample with the smallest gap in the real data, and take its corresponding calculation object sample as the y_{n+1} calculation value. According to the similarity calculation principle, the error value is the smallest. Select the calculation object sample corresponding to the first K minimum distance samples, and implement weight estimation for the real-time calculation results. The expression is:

$$y'_{n+1} = \sum_{j=1}^{K} W_{j(n+1)} y_j \quad (7)$$

In Formula (7), K represents the number of nearest neighbors, y_j represents the nearest neighbor history calculation object sample, and $W_{j(n+1)}$ represents the weight coefficient corresponding to y_j. K is usually taken based on the number of samples n. The $W_{j(n+1)}$ selection principle is that the distance and the extraction weight are inversely proportional. The smaller the distance, the greater is the weight value.

When using the NNBR model to measure and calculate the surface settlement due to the construction of a tunnelling shield,the tunnelling depth and average tunnelling speed are taken as the calculation factors, and the calculation factor set is constructed. Taking the settlement value of the middle line of the tunnel as the calculation object, the historical calculation samples and historical calculation object samples are constructed according to the above survey data.

3.2 Program Design for Regional Surface Deformation Monitoring

According to the calculation principle of GNSS and satellite signal processing, through VC6 0 design the calculation and analysis program of surface deformation of underground

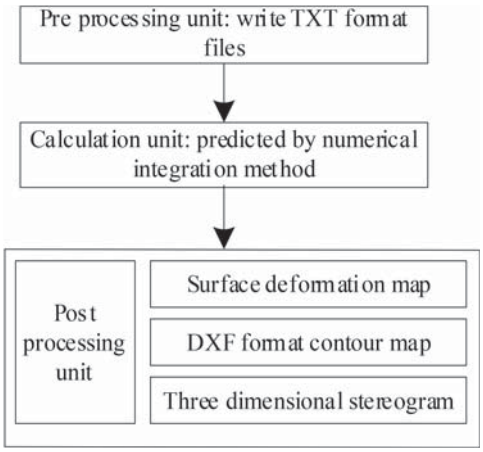

Figure 3 Regional surface deformation monitoring procedure.

Table 2 Inspection level of monitoring results.

Grade	Calculate a posteriori value	Probability error
1	0.35	0.95
2	0.50	0.85
3	0.75	0.75
4	0.90	0.65

mining, and the design results of the program are shown in Figure 3.

In Figure 3, the pre-processing unit is responsible for compiling the calculation file in TXT format, inputting parameters such as the conditions required for regional surface deformation monitoring, and then starting the program to calculate the surface deformation parameters through GNSS and satellite signal processing prior to monitoring the deformation.After the monitoring, enter the post-processing unit and save it as a MATLAB graphic file according to the measured surface deformation value. At the same time, the contour map can be drawn according to the monitoring deformation results and output in the form of a DXF file using Auto CAD software. The surface deformation results can also be output as a MATLAB three-dimensional graphics file.

In order to eliminate the influence of dimensional differences, it is necessary to standardize all calculation factors. The processing formula is:

$$x'_{ik} = \frac{x_{ik} - \overline{x}_k}{S_k} \tag{8}$$

In Formula (8), x'_{ik} represents the k calculation factor in the i historical sample after standardization.According to the standardized data, use Formula (8) to obtain the final settlement result. The monitoring time series can be obtained through this formula. Testing is required to evaluate and improve the monitoring accuracy of the model. According to the application requirements of the design monitoring method, the residual method is used for secondary calculation, and the model residual is set as $\alpha(k)$. The calculation formula can be written as follows:

$$\alpha(k) = a^{(1)k} - a^{(1)}(k+1) \tag{9}$$

Based on the above analysis, the detailed operation steps of regional surface deformation monitoring method are obtained as follows:

(1) Set the bilateral filter function and the corresponding range, and also set the corresponding airspace and range variance [15].

(2) Set a $\gamma = P_i/2T$;

(3) The type of image data acquired;

(4) Gaussian simulation method is used to simulate the data and accumulate the simulated data.

(5) According to the data obtained by cumulative superposition, the above data are processed by bilateral filtering to obtain the data after denoising, and the regional surface deformation monitoring is completed.

Through the above steps, verify the authenticity and reliability of the monitoring results, and divide the obtained calculated posterior value and probability error level as shown in Table 2.

According to the above classification results, the results obtained by the monitoring method are divided to improve the surface settlement monitoring results. This completes the design of a regional surface deformation monitoring method based on GNSS and satellite signal processing.

4. EXPERIMENTAL ANALYSIS

The monitoring performance of this method is verified by simulation, which requires staff to collect relevant data on site. However, there are many uncertain factors, and it is also limited by the on-site collection environment, which

Table 3 Summary of tunnel section data.

Tunnel section number	Dongji n/m	Overburden thickness/m	Excavation area/m^2	Average denstiy g/m^3	Deformation modulus/Mpa
ST12+501	6.25	5.34	36.15	1.66	1.56
ST12+502	6.15	5.14	36.00	1.87	1.67
ST12+503	6.34	5.24	36.28	1.82	1.84
ST12+504	6.14	5.60	36.47	1.74	1.74
ST12+505	6.00	5.14	36.85	1.51	1.68

Table 4 Monitoring error analysis.

Monitoring location	Subsidence value/mm		Curvature value/10^{-3}		Tilt valuemm/m	
	Measured value	Monitoring value	Measured value	Monitoring value	Measured value	Monitoring value
Position 1	299	299	1.98	1.98	0.090	0.090
Position 2	287	287	1.59	1.59	0.146	0.146
Position 3	324	324	1.98	1.98	0.136	0.136
Position 4	364	362	1.68	1.67	0.143	0.143
Position 5	357	357	1.76	1.75	0.178	0.178
Position 6	447	447	1.90	1.90	0.136	0.134
Position 7	367	367	2.33	2.33	0.107	0.107
Position 8	379	379	1.50	1.50	0.109	0.109
Position 9	268	266	1.89	1.89	0.106	0.105
Position 10	364	364	1.58	1.59	0.108	0.108

makes it impossible to obtain on-line monitoring data, and the monitoring efficiency is low. However, the method designed in this paper adopts GNSS and satellite signal processing technology to make use of its ideal transmission rate and real-time, on-line characteristics. Through the network server, the staff can monitor the regional surface data and the operation status of the monitoring equipment in real time. If the monitoring equipment fails, the staff may receive relevant abnormal data to judge the cause of the failure, send maintenance personnel for maintenance in time, and monitor and master the data of runoff and sediment in real time. If large fluctuations are found in the data, the water situation and soil loss can be judged, so that appropriate preventive measures can be taken in time. Compared with the existing monitoring methods, it has more real-time and improves the efficiency of monitoring. In this experiment, the tunnel is preset as a new construction section of a high-speed railway, and five test sections are set as data samples in this section. The specific tunnel section data is summarized in Table 3.

Taking the above data as an example in this experiment, this method and the other two monitoring methods are used to monitor the surface settlement, and the monitoring results are analyzed.

In this experiment, the monitoring errors of the three monitoring methods, the vertical displacement at different mining depths, the horizontal displacement at different mining depths and the surface settlement monitoring of regional shield tunnel will be measured and compared. In the experiment, the calculation formula for the monitoring error is:

$$W_{cw} = \left| \frac{J_j - C_c}{C_c} \right| \times 100\% \tag{10}$$

In Formula (10), J_j represents the measured value, C_c represents the output value of the monitoring method, and W_m represents the relative error.

In the experiment used to test the vertical displacement and horizontal displacement at different mining depths, in order to improve the authenticity of the monitoring method results and for comparison purposes, three mining depths were considered: 20m, 40m and 60m. By calculating the three comparison indexes above, the corresponding data are obtained to evaluate the method proposed in this paper.

When testing the surface settlement monitoring results obtained fora regional tunnelling shield, it shall be verified according to the regional surface settlement monitoring value and real value.

Ten surface test points are selected and the discrepancy between the measured value and monitored value of surface deformation data obtained by the proposed method is analyzed. The analysis results are shown in Table 4.

According to Table 4, among the subsidence values monitored by this method, only position 4 and position 9 have small errors, and the maximum error is only 2mm. The monitored curvature value has errors only in position 4, position 5 and position 10. In the monitoring of tilt value, the error is still relatively small, the highest is only 0.002m, which shows that the monitoring results obtained by this method have only a small error.

The surface vertical displacement curve is obtained for different mining depths, and the monitoring effect obtained by the proposed method is analyzed. The experimental results are shown in Figure 4.

As shown in Figure 4, when the mining depth is 20m, the change of vertical displacement is higher than that at 40m and 60m. When the mining depth is 60m, there is least change in vertical displacement,indicating that the greater the mining depth, the less is the change in vertical displacement. Moreover, when monitoring surface vertical displacement and deformation by this method, the monitoring results are very close to the measured value of vertical displacement,

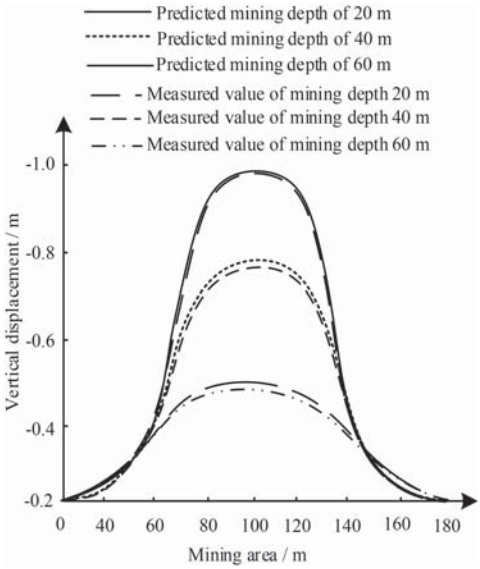

Figure 4 Vertical displacement at different mining depths.

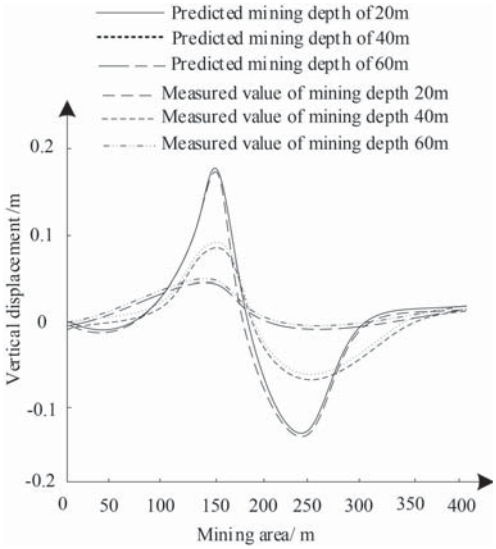

Figure 5 Horizontal displacement at different mining depths.

and there is no significant change. Therefore, this method is very accurate when monitoring vertical displacement and deformation.

The surface horizontal displacement curve under different mining depths is analyzed, and the monitoring results obtained by the proposed method are examined. The experimental results are shown in Figure 5.

According to Figure 5, the greater the mining depth, the smaller is the horizontal displacement deformation fluctuation of the surface. When the mining depth is 20m, the horizontal displacement fluctuates within about 0.2m∼–0.2m. When the mining depth reaches 60m, the horizontal displacement fluctuates within about 0.05m∼–0.05m. The results obtained by the proposed method closely approximate the actual mining situation, and there is still no large error. Therefore, this method is highly accurate when used to monitor horizontal surface displacement.

The monitoring performance of the proposed method is tested, and the measured value and monitoring value change of the section in the monitoring area are analyzed. The specific experimental results are shown in Figure 6.

By analyzing the experimental data depicted in Figure 6, it can be seen that the regional surface settlement monitoring value obtained by this method is basically consistent with the real value, which comprehensively confirms the superior performance of the proposed method.

5. CONCLUSION AND FUTURE WORK

5.1 Conclusion

(1) The monitoring results of regional surface deformation monitoring method based on GNSS and satellite signal processing have small errors.

(2) In the process of monitoring surface vertical displacement and deformation by this method, the monitoring

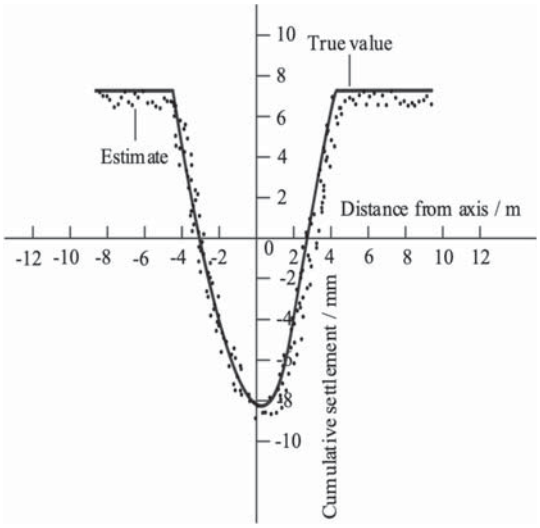

Figure 6 Test results of surface settlement monitoring of regional tunnelling shield.

value in this paper is very close to the measured value of vertical displacement, and there is no significant change. This method is very effective for monitoring vertical displacement and deformation.

(3) The monitoring results obtained by the proposed method are very consistent with the actual mining situation, and there is still no large error. Therefore, this method can monitor surface horizontal displacement with high accuracy.

(4) The monitoring value of regional surface subsidence obtained by this method is basically consistent with the real value, which confirms the superior performance of this method.

5.2 Future Work

Since not all design issues have been thoroughly considered,further work is required to improve the proposed monitoring system.

(1) Previous research shows that, compared with the obvious topographic deformation caused by an earthquake with its particular characteristics and effects, the amount of surface subsidence caused by mining in some mining areas is relatively small, and the surface deformation in some mining areas is very slow. Because this deformation data is weak, and the measurement accuracy of inertial device sensor cannot meet the corresponding requirements, it is difficult to measure deformation accurately.

(2) As an auxiliary optical fiber strain sensor for regional Terrain Deformation Monitoring, there are also corresponding optimization problems in the layout of its measurement network sensors. In the overall design of the deformation monitoring system, it is necessary to consider the optimal number of measurement sensors to be deployed, and at the same time, it is also necessary to consider how to design the monitoring network to optimize the measurement effect, which needs to be verified repeatedly by measuring the actual deformation, which is difficult to achieve. This will be a focus of future research work.

(3) When dealing with non-stationary signals, wavelet transform can choose a variety of wavelet basis functions. However, once the wavelet basis has been selected, its characteristics will be fixed. Each time the wavelet is decomposed on each scale, the detail length and approximation signal will be reduced by half. There are always some differences between the data of wavelet signals for different scales. It is difficult to accurately describe some local characteristics of data signals when wavelet transform is carried out. Therefore, the selection of the most appropriate wavelet base will be the focus of repeated experiments in future work.

(4) In the segmentation mode representation of time series, two endpoints in the segmentation continuity need to be considered. If more sequence points of multiple sequences and their subsequences coincide, the accuracy of segmentation will be strengthened. Therefore, it is very important to select appropriate data segmentation points.Extending the continuous condition to smooth continuity can further improve the expression ability of data morphology.

REFERENCES

1. Mirmazloumi SM, Barra A, Crosetto M, Monserrat O, Crippa B. Pyrenees deformation monitoring using sentinel-l data and the persistent scatterer interferometry technique. *Procedia Computer Science*. 2021; 181: 671–677.
2. Kamali ME, Papoutsis I, Loupasakis C, Abuelgasim A, Omari K, Kontoes C. Monitoring of land surface subsidence using persistent scatterer interferometry techniques and ground truth data in arid and semi-arid regions, the case of Remah, UAE. *Science of The Total Environment*. 2021; 776: 145946.

3. Cigna F, Tapete D. Present-day land subsidence rates, surface faulting hazard and risk in Mexico City with 2014–2020 sentinel-l IW InSAR. *Remote Sensing of Environment*. 2020; 253: 112161.
4. Jowitt PW. Systems and sustainability: sustainable development, civil engineering and the formation of the civil engineer. *Civil Engineering and Environmental Systems*. 2020; 37(4): 79–88.
5. Hakim WL, Achmad AR, Eom J, Lee CW Land subsidence measurement of Jakarta coastal area using time series interferometry with sentinel-l SAR data. *Journal of Coastal Research*. 2020; 102(Sl): 75–81.
6. Berardino P Fornaro G, Lanari R, Sansosti E. A new algorithm for surface deformation monitoring based on small baseline diff erential SAR interferograms. *IEEE Transactions on Geoscience & Remote Sensing*. 2002; 40(11): 2375–2383.
7. Aldao E, González-Jorge H,Pérez JA. Metrological comparison of lidar and photogrammetric systems for deformation monitoring of aerospace parts. *Measurement*. 2021; 174: 109037.
8. Nemah HA, Ahmed MM, Khaleed OL, Nemat GS. Eff ect of some meteorological variables and conditions on mobile phone and 'tv' satellite signal. *Al-Mustansiriyah Journal of Science*. 2021; 32(2): 71–80.
9. Park G, Lee B, Kim DG, Lee YJ, Sung S. Design and analysis of map interacted integrated navigation system under urban environment with constrained satellite signal. *Journal of Institute of Control*. 2020; 26(5): 392–397.
10. Nian FD, Li T, Bao BK, Xu CS. Relative coordinates constraint for face alignment. *Neurocomputing*. 2020; 395: 119–127.
11. Nomura H,Tsukagoshi T, Kawabe R, Muto T, Kanagawa KD, Aikawa Y, et al. High spatial resolution observations of molecular lines towards the protoplanetary disk around TW Hya with ALMA. *The Astrophysical Journal*. 2021; 914(2): 113–120.
12. Zhang XN, Zhang SF High-precision indoor dynamic target positioning method based on GNSS/SLAM combination. *Computer Simulation*. 2021; 38(3): 465–469.
13. Zvirgzds J, Celms A.GNSS RTK performance improvements using Galileo satellite signal. *Latvian Journal of Physics and Technical Sciences*. 2020; 57(1–2): 78–84.
14. Noel SA, Ault AA, Buckmaster DR, Krogmeier JV A rainfall-based, sequential depression -filling algorithm and assessments on a watershed in northeastern Indiana, USA. *Journal of Advances in Modeling Earth Systems*. 2021; 13(6):eMS002362.
15. Joshi K, Diwakar M, Joshi NK, Gupta H, Baloni D. Cross bilateral filterbased image fusion in transform domain. *SSRN Electronic Journal*. 2020; 2(3): 1–7.